Acta Crystallographica Section B
Structural Science
ISSN 0108-7681

Structure and intermolecular interactions of glipizide from laboratory X-ray powder diffraction

Jonathan C. Burley

University Chemical Laboratory, Lensfield Road, Cambridge CB2 1EW, England

Correspondence e-mail: jb442@cam.ac.uk

Received 7 March 2005
Accepted 15 August 2005

The crystal structure of glipizide, used as a major treatment of type-2 diabetes, has been determined *ab initio* using variable-temperature laboratory X-ray powder diffraction combined with a direct-space Monte Carlo/simulated annealing methodology. The strengths of the intermolecular interactions (van der Waals, π–π stacking, hydrogen bonding and steric interlock) were quantitatively estimated using the thermal expansion data, which were collected in the same set of experiments as those used to determine the structure.

1. Introduction

Although molecular structures and crystal packing can be quantitatively determined with considerable accuracy, the forces and interactions which lead to the formation of the crystals are generally inferred qualitatively from the crystal structure itself. Short intermolecular distances are taken as indications of the presence of strong interactions, while longer distances are taken to indicate that an interaction is weak. The validity of this approach has been questioned (for a recent review, see Dunitz & Gavezzotti, 2005). Calculations of intermolecular interactions are often useful to rationalize the data, but, although being very powerful, are not at present sufficiently reliable for the unambiguous prediction of crystal structures (Lommerse *et al.*, 2000). An improved method of experimentally determining intermolecular forces is thus of great importance, in the context of crystal structure prediction, property rationalization and in other areas in which intermolecular interactions determine the chemistry and properties of a material.

It is well known that significant qualitative information on intermolecular interactions can be determined from the thermal expansion of a material. For example, the fact that most materials expand on heating indicates that the model of a simple harmonic oscillator moving in a symmetric potential cannot be a good description of intermolecular interactions because in the simple harmonic oscillator the intermolecular distances are temperature invariant. As a result, various asymmetric forms of the potential (*e.g.* Morse, Lennard–Jones, exp-6) have been proposed and are widely employed in modelling the properties of isolated molecules, liquids and solids. Typical examples of solids for which the thermal expansion has been studied in this context include alumina, rutile, solid noble gases and particularly the alkali halides (Ruffa, 1980; Wang & Reeber, 2000; Barron, 1955). However, there are very few examples in the literature of the quantitative analysis of the thermal expansion data of molecular materials, although work based on lattice parameters derived from high-resolution neutron diffraction on C_{60} indicated that

a surprising amount of information can be extracted (David *et al.*, 1993).

A typical model used to describe the thermal expansion of solids comprises a small number of Einstein terms which very crudely approximate the vibrational spectrum (Wang & Reeber, 2000). This model is particularly attractive as each of the different vibrational terms is characterized by a single Einstein temperature, θ, which describes the 'lattice stiffness' (taken here to indicate an estimate of the interaction energy between atoms or molecules in the crystal) and the term X_j, which includes a number of contributions including a Grüneisen-like term. The physical significance of the sign of X_j (and hence the Grüneisen-like term) is that it defines the sign of the anharmonicity of the lattice potential (Munn, 1975; Zallen, 1974).

In this paper this simple model is applied to the anisotropic thermal expansion in the title compound glipizide and it will be shown that chemically reasonable and quantitative values for interactions between molecules can be determined. This is achieved by assigning the phonon terms microscopically to particular interactions; a similar approach has been demonstrated for ZrW_2O_8, in which the hopping energy for an oxide-ion migration was determined from thermal expansion data (Evans *et al.*, 1999). Although the model employed in the present work is extremely simple, involving only four vibrational terms for the entire crystal, it should be noted that in the solid state the forces between molecules are typically described qualitatively in terms of a small number of interaction terms, such as hydrogen-bond networks, π–π stacking and the like. The crystal structure of glipizide is also presented for the first time – this was determined from variable-temperature laboratory X-ray powder diffraction data. A new and simple procedure for indexing complex unit cells is also briefly presented.

2. Experimental

2.1. Indexing and structure solution

Glipizide (also known as glucotrol) was purchased from Acros (USP grade) and was used as received. X-ray powder diffraction data were collected using Co $K\alpha_1$ radiation (λ = 1.79 Å) on a Stoe Stadi-P diffractometer operating in Debye–Scherrer geometry; the sample was contained in a 0.7 mm diameter capillary. Datasets with relatively high signal:noise ratios, suitable for structure solution, were collected at 290 and 125 K (approximate counting time: 24 h per data set), and with lower signal:noise ratios, suitable for the determination of lattice parameters through a Rietveld analysis, every 5 K from 150 to 380 K (approximately 1 h per dataset). No phase transition was apparent from the variable-temperature data.

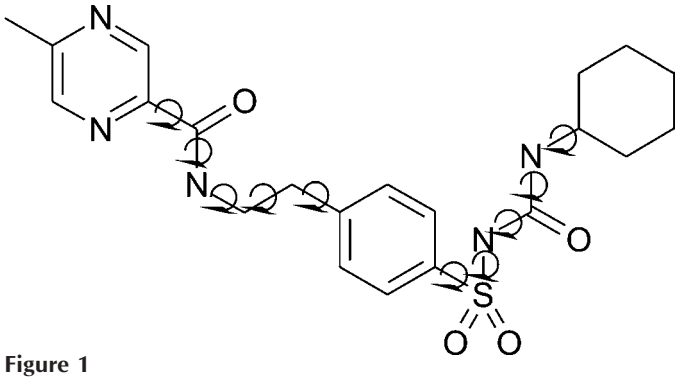

Figure 1
Molecular structure and available torsion angles for glipizide.

Preliminary attempts to index the pattern at 295 K were not successful – several different monoclinic and triclinic cells of reasonable density were available with acceptable figures of merit (*e.g.* at room temperature: F_{18} = 50 for a monoclinic cell of density 18 Å^3 per non-H atom, F_{18} = 54 for a larger monoclinic cell of density 14.9 Å^3 per non-H atom) and were not easily distinguished through whole-pattern fitting. The interface *CMPR* was used for indexing, along with the included standard peak-fitting routines and indexing software, namely the Finger–Cox–Jephson modified pseudo-Voigt, *TREOR* and *DICVOL*, respectively (Finger *et al.*, 1994; Werner *et al.*, 1985; Boultif & Louer, 1991). Attempts were made to index the pattern at each temperature over the entire temperature range using between 15 and 25 peaks per temperature as appropriate. Out of numerous possible cells suggested by the indexing routines, it was found that only one was suggested repeatedly across the entire temperature profile and could be used to account for the pattern at all temperatures. Note that this cell was not amongst those suggested in the initial indexing of the room temperature high signal:noise dataset, although subsequent work indicated that it could fully account for all peaks observed in that pattern. Thus, the use of variable-temperature data analysis allowed for a rapid evaluation of the most probable unit cell and this was selected for further analysis (space group $P\overline{1}$, $a \simeq 9$, $b \simeq 24$, $c \simeq 5$ Å, $\alpha \simeq 93$, $\beta \simeq 101$, $\gamma = 83^\circ$, $V \simeq 1100$ Å^3, $Z = 2$, $Z' = 1$). The experimental details are given in Table 1.[1]

Using this cell, *hkl* intensities were extracted at 295 and 125 K using the Le Bail algorithm (Le Bail *et al.*, 1988; at room temperature, R_{wp} = 0.0464, R_p = 0.0366) and repeated attempts were made to solve the stucture using the Monte Carlo/simulated annealing (MCSA) method, as implemented within *PSSP* (Stephens & Huq, 2002) employing ten torsion angles and six variables to describe molecular position and orientation (Fig. 1). The first 150 reflections ($d \geq 2.44$ Å) were used. The molecular model was constructed using standard methods. A fully reproducible minimum in the goodness-of-fit S was not located using the room-temperature data, however, the use of *hkl* intensities extracted from the 125 K data set did allow a reproducible minimum to be located with 9 out of 10 runs (T = 50–0.0001, cooling rate 2% per temperature, 1 million trial structures per temperature, random starting values for structural parameters) converging to give S = 0.003 (where S = 0.000 represents an excellent fit). Rietveld refinements were performed within the *GSAS* program suite (Larson & Von

[1] Supplementary data for this paper are available from the IUCr electronic archives (Reference: AV5037). Services for accessing these data are described at the back of the journal.

Table 1
Experimental details.

Crystal data	
Formula	$C_{21}H_{27}N_5O_4S$
M_r	445.06
Crystal system	Triclinic
Space group	$P\overline{1}$
a (Å)	9.1487 (3)
b (Å)	24.2873 (8)
c (Å)	5.1794 (1)
α (°)	93.118 (3)
β (°)	101.154 (2)
γ (°)	83.479 (2)
V (Å^3)	1121.20 (7)
Z	2
D_x (Mg cm^{-3})	1.318
μ (mm^{-1})	0
2θ range (°)	2–79.99
Step size (° 2θ)	0.01
Wavelength (Å)	1.79
No. of profile data steps	7800
No. of contributing reflections	798
No. of structural variables	200
No. of profile parameters	2
No. of bond-length constraints	60
No. of bond-angle constraints	106
No. of planar group constraints	2
R_p	0.0383
R_{wp}	0.0500
R_{exp}	0.0369
χ^2	2.026
R_B	0.0541

Dreele, 1990) on all data sets over the entire temperature range and converged readily to yield acceptable goodness-of-fit values (*e.g.* $R_{wp} = 0.232$, $R_p = 0.165$, $\chi^2 = 3.18$ at 175 K, a low signal:noise dataset) and visually acceptable fits. Restraints on bond angles, bond lengths and planar groups were input based on molecular fragments taken from the CSD (Allen, 2002). Restraints were heavily weighted and a single atomic displacement parameter (ADP) was employed. H atoms were included at calculated positions and subjected to restraints. A shifted Chebyshev polynomial was used to model the background, with a Finger–Cox–Jephson modified pseudo-Voigt function to model the peak profile. No evidence of any significant preferred orientation was apparent from trial refinements. The N and C atoms could not be distinguished in the pyrazyl rings due to the near-equivalence of electron count and were arbitrarily assigned. At room temperature (high signal:noise data set), $R_{wp} = 0.050$, $R_p = 0.0383$, $R_{Bragg} = 0.0541$ and $\chi^2 = 2.026$ (Fig. 2): $P\overline{1}$, $a = 9.1488$ (3), $b = 24.2871$ (8), $c = 5.1795$ (1) Å, $\alpha = 93.118$ (3), $\beta = 101.154$ (2), $\gamma = 83.479$ (2)°, $V = 1122.20$ (7) Å^3, $Z = 2$, $Z' = 1$. The derived structural parameters have been deposited and the crystal structure shown in Fig. 3.

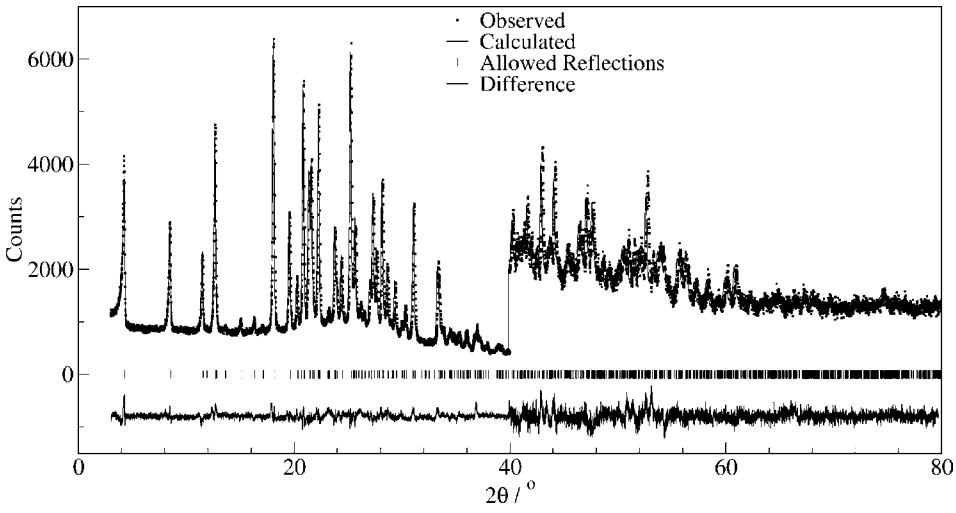

Figure 2
Rietveld refinement of glipizide at room temperature. The trace above 40° is multiplied by a factor of five.

2.2. Determination of intermolecular forces

The simple model to describe thermal expansion, presented above (Wang & Reeber, 2000), was fit to the Rietveld-derived lattice parameters in the temperature range 150–375 K (Fig. 4, Table 2). The approximation is made that this approach is a reasonable method of studying the interactions between molecules because these interactions are aligned along the crystallographic axes. For example, the hydrogen-bonding network runs in the **a** direction. The overall approach is equivalent, in the present case, to modelling the variation in molecular separation as a function of temperature, in the directions in which the strongest intermolecular interactions are expected. As these interactions are not orthogonal the derived values do not represent true independent vibration modes, but are expected instead to provide a reasonable approximation of these intermolecular interactions. Attempts were also made to analyse the expansion using a tensor approach (decomposition of the thermal expansion into primary components *via* the usual eigenvalue procedure) using both literature methods (Schlenker *et al.*, 1978; Paufler & Weber, 1999). Neither proved satisfactory in terms of producing robust, reliable tensors and the conclusions of Paufler and Weber apply here: namely that 'thermal expansion coefficients of triclinic crystals seem to be particularly sensitive to the exact procedure of evaluation'. However, the main aim of this work is to demonstrate that a simple model can be successfully used to analyse the lattice expansion of complex molecular crystal structures quantitatively in terms of a limited number of chemically reasonable interactions between molecules and as such a full description of the thermal expansion in terms of a tensor is not essential. It was assumed that the intramolecular bond lengths were temperature invariant, as is usually observed for molecular materials,

and that no significant molecular reorientations occurred in the temperature range studied. The latter assumption appears reasonable given that refinements over the entire temperature range give no indication of any such reorientation. Note also that the model assumes that for each term the Grüneisen parameter is temperature independent – although this is not likely to be strictly the case, Grüneisen parameters do not typically vary greatly from a value of *ca* 2 as a function of temperature for $T > 0.2\theta$ (Krishnan *et al.*, 1979). The model fits clearly describe the data satisfactorily, as well as producing reasonable numerical values for the energies of interaction.

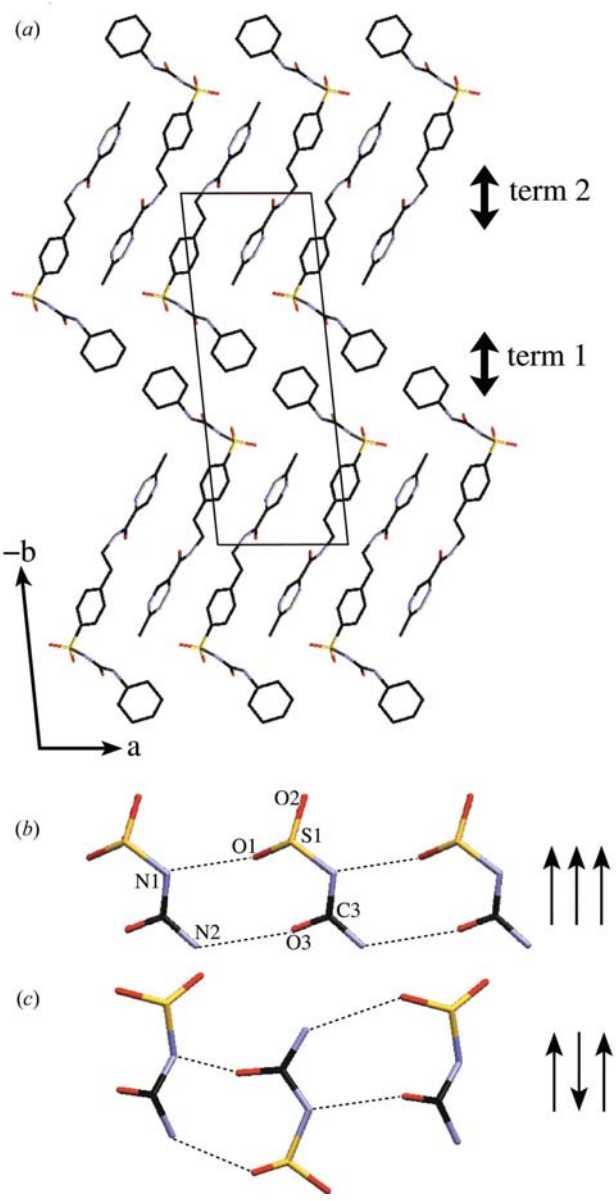

Figure 3
(*a*) Crystal structure of glipizide. A chain of hydrogen bonds runs into the page. Double-headed arrows indicate the two vibrational terms present along **b**. (*b*) $R_2^2(10)$ hydrogen-bond network in glipizide, and the *A* polymorph of acetohexamide (Stephenson *et al.*, 1997). (*c*) Hydrogen-bond network in 1-isopropyl-3-(4-(3-chlorophenylthio)-pyrid-3-yl)sulfonylurea (Dupont *et al.*, 1979), and in the *B* polymorph of acetohexamide (Stephenson, 2000). For (*b*) and (*c*), the single-headed arrows arrows indicate the fragment orientation.

Table 2
Coefficients used to model the anisotropic thermal expansion of glipizide.

The model used was $\ln(l_{calc}) = \ln(l_0) + [X_1\theta_1/(\exp(\theta_1/T) - 1)] + [X_2\theta_2/(\exp(\theta_2/T) - 1)]$, where l_{calc} is the calculated lattice parameter and l_0 the extrapolated 0 K value, X_i a coefficient which includes the effects of the Grüneisen parameter, density of states, bulk modulus and volume, and θ_i is the term frequency. Standard uncertainties are given in brackets.

Parameter	l_0 (Å)	θ_1 (K)	$X_1 \times 10^{-5}$	θ_2 (K)	$X_2 \times 10^{-5}$
a	9.026 (3)	532 (30)	12.8 (4.8)	–	–
b	24.044†	388 (56)	7.8 (1.8)	1464 (340)	−21.0 (7)
c	5.1591 (7)	850 (78)	5.15 (0.67)	–	–

† In order to reduce the number of variables for the two term fit, l_0 for **b** was fixed at 24.044 Å, a value determined through trial fits.

Both of these facts are taken to indicate that the model is at the very least useful for the purposes of discussion. Without further examples of this approach it cannot be stated unambiguously that the model is a good description of the essential physics involved, but the model does provide excellent rationalization of the intermolecular interactions in the present case.

3. Discussion

Despite the use of both the *DICVOL* (Werner *et al.*, 1985) and *TREOR* (Boultif & Louer, 1991) indexing programs, the room-temperature, high signal:noise pattern could not initially be indexed correctly. The use of variable-temperature data allowed a rapid and reliable determination of the most probable unit cell. The fact that one unit cell can index the patterns over the entire temperature range increases confidence that the correct unit cell has been determined. This is a very simple and intuitive strategy, although it does not seem to have been applied to date. Several examples exist of the use of variable-temperature studies, coupled with anisotropic cell expansion, being used to extract peak intensities for input into direct methods or other structure solution techniques (Shankland *et al.*, 1997; Brunelli *et al.*, 2003; David *et al.*, 2002; Zachariasen & Ellinger, 1963). However, the use of variable temperature for indexing purposes appears to be new. Clearly, for materials in which no phase transition occurs in the temperature range investigated, this method is likely to be generally applicable.

During the process of MCSA structure solution it became clear that the *hkl* intensities extracted at 295 K were not sufficiently reliable for a reproducible minimum in the goodness-of-fit hypersurface, presumably due to unresolved peak overlap. Intensity extraction using the 125 K dataset surmounted this problem and thus allowed a full and reliable structure determination. It should be noted that the greater ease of structure determination at low temperatures is *not* due to decreased ADPs on the atoms and concomitant extension of Bragg scattering at high angles (as is frequently encountered using direct methods in single-crystal studies) – for the structure solution step, only relatively low-angle data were used. Thus, for both indexing and structure solution the use of

variable-temperature data were essential given that a laboratory instrument was used.

The crystal structure of glipizide (Fig. 3) consists of layers formed by pairs of sterically interlocking molecules – the layers are aligned perpendicular to **b**. These layers are linked by van der Waals interactions at the point of contact of the cyclohexyl rings. Along **a**, π–π interactions appear to be present, with phenyl–pyrazyl subunits in adjacent molecules arranged in an offset face-to-face manner. Along **c**, $R_2^2(10)$ hydrogen-bonded dimeric rings and $C_1^1(3)$ chains form two parallel infinite chains of intermolecular hydrogen bonds. Relevant distances at room temperature for the $R_2^2(10)$ network are 2.983 (4) Å for O1···N1 and 2.979 (4) Å for O3···N2, with the $C_1^1(3)$ network being formed by an N3···O4 interaction of 2.972 (3) Å (standard uncertainties are taken from the Rietveld program employed). The pattern of the hydrogen bonding is similar to that observed in a number of sulphonylureas, for which two main patterns are observed, one in which the sulphonylurea fragments are arranged in a parallel manner, and another in which the fragments are antiparallel (Figs. 3*b* and *c*, respectively). In glipizide the parallel configuration is observed – acetohexamide is an example of a compound exhibiting polymorphism which appears to be driven by the small energy separation of the two configurations (Stephenson, 2000; Stephenson *et al.*, 1997). The C14···C14 intermolecular distance is the only one (apart from H···H contacts) which is less than the sum of the van der Waals radii at 3.329 (9) Å (compared with the van der Waal's value of 3.4 Å). A search of the Cambridge Crystallographic Database indicates that this distance is reasonable – of 767 entries in which a carbon of an amide α to the nitrogen has a short intermolecular contact (less than the sum of VdW radii) with another carbon, 319 have distances 3.301–3.375 Å, with 207 entries having intermolecular contacts even shorter than this. The intramolecular bond lengths fall within the expected ranges (they were subject to restraints). The refined atomic displacement parameter is positive and assumes a reasonable value. In short, the refined crystal structure is chemically and crystallographically reasonable.

If the thermal expansion of the lattice can be used as a reasonable probe of the interactions between molecules, the thermal expansion of glipizide might be expected to be highly anisotropic and of the order $a > b > c$, *i.e.* interaction energies between molecules in the order hydrogen bonding > (van der Waals + steric interlock) > π–π. Comparison of the cell dimensions at 290 and 125 K reveals that the percentage expansion is in the approximate ratio 10:5:1, *i.e.* fully in keeping with the intermolecular interactions expected based on consideration of the refined crystal structure.

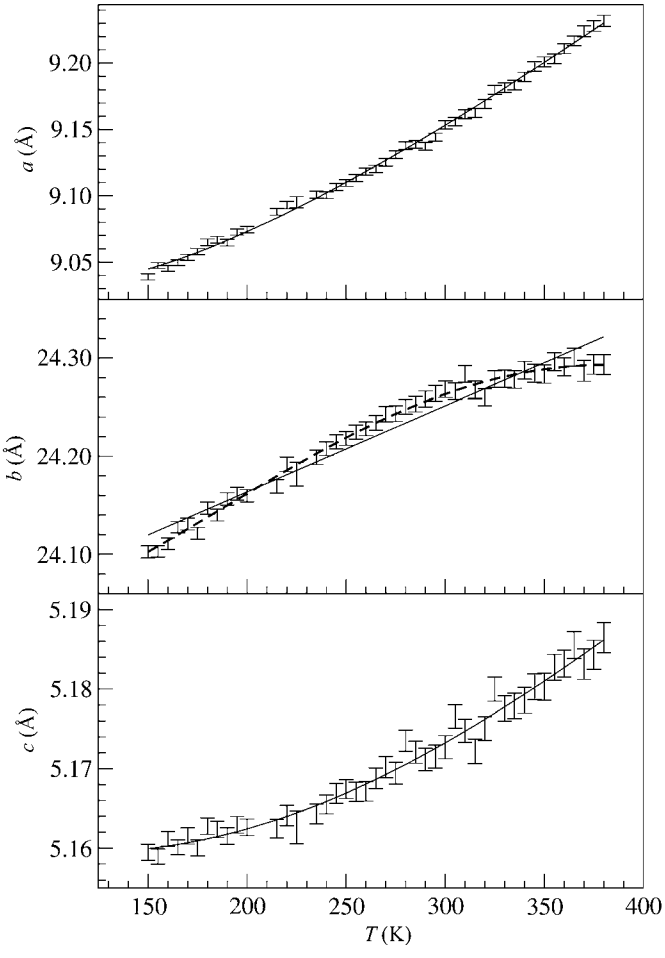

Figure 4
Thermal expansion of glipizide. The solid lines are fits to a single-term phonon-driven expansion, with the dashed line being a fit to a dual-term model.

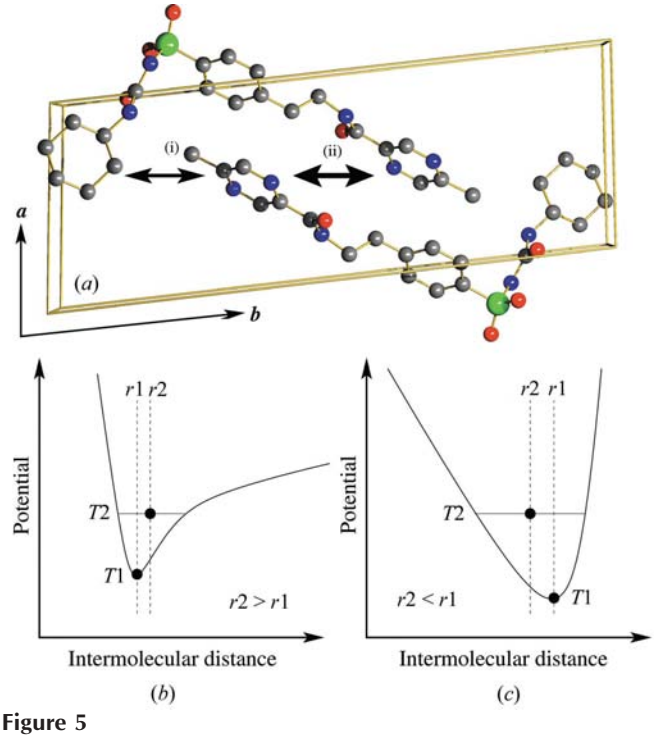

Figure 5
(*a*) Detailed view of the interlocking interaction along **b** between glipizide molecules. The repulsion at (ii) is greater than that at (i) and leads to a negative contribution to the thermal expansion along **b**. (*b*) Schematic of a standard intermolecular potential, leading to positive thermal expansion. (*c*) Schematic of a possible intermolecular potential for term 2, leading to negative thermal expansion. For (*b*) and (*c*), the temperature T_1 is less than T_2.

It is well established that for structurally anisotopic materials, successfully modelling heat capacity or thermal expansion requires a number of Einstein terms. For example, as early as 1911 Nernst suggested that two Einstein modes, once corresponding to an in-layer displacement and another to a displacement perpendicular to the layer, were required to model the heat capacity of graphite (*e.g.* Nernst, 1911). Likewise, several Einstein modes are required to model the thermal expansion of sodium chloride across a wide temperature range. In the present case, successfully modelling the anisotropic thermal expansion of the title compound, glipizide, using the equation of Wang & Reeber (2000), requires four Einstein terms. The four terms can easily be assigned to particular interactions in the crystal structure, corresponding to those which would be used to discuss the intermolecular interactions in a qualitative manner. In the **a** direction, where a single type of interaction ($\pi\cdots\pi$) is predicted, a model involving a single intermolecular interaction is sufficient to account for the thermal expansion. Likewise, along **c** a single interaction corresponding to the infinite-chain hydrogen-bonding network accurately models the experimental data. These single vibrational terms along **a** and **c** both drive a positive thermal expansion (as X_1 is positive), and the relative strengths of the interactions, as inferred from the Einstein temperatures, are in agreement with the hydrogen-bonding interactions ($\theta \simeq 850$ K) being stronger thatn the $\pi\cdots\pi$ interactions ($\theta \simeq 532$ K). In contrast, along the **b** direction the thermal expansion cannot be modelled using a single interaction term. Rather, two terms are required. The first is a low-energy term ($\theta \simeq 388$ K) which drives a positive contribution to the overall lattice expansion in this direction – qualitatively, it is easy to see that this is the lower-energy term as the expansion is greater at lower temperatures where this positive thermal expansion term dominates. The second term (with negative X_2) drives a negative contribution to the expansion and is of very high energy ($\theta \simeq 1464$ K) – again this can be easily seen from a form of the $\mathbf{b}(T)$ curve with a reduction in expansion, driven by this negative thermal expansion term, setting in at higher temperatures (Fig. 4). The fact that this term begins to dominate at high temperatures indicates that it is not a simple transverse oscillation which drives the low-temperature negative thermal expansion in silicon, for example (Biernacki & Scheffler, 1989). Bond bending is generally of far lower energy than bond stretching and thus a term involving transverse oscillations would be expected to occur at far lower temperatures than the term with positive X_j. The opposite is observed.

The first term used to describe the thermal expansion in the **b** direction can be assigned (term 1, Fig. 3) to the interaction between molecules at the point of contact of the cyclohexyl rings, as this is expected to be a low-energy van de Waals interaction. The second term (term 2, Fig. 3) is assigned to a vibration in which sterically interlocked molecules try to move apart parallel to **b** – this is indicated schematically in Fig. 5. This movement of the molecules is naturally very energetically unfavourable as it involves the molecules moving through each other, and being structurally frustrated it is reasonable that this drives a negative contribution to the expansion (Mary *et al.*, 1996). Negative thermal expansion in the present case is caused by repulsion (ii) in Fig. 5(*a*) being greater than repulsion (i). This leads to the vibrational term 2 along **b** (the term due to interlocking molecules) tending to cause a contraction of the lattice in that direction. It should be noted that for all standard intermolecular potentials (Morse, Lennard–Jones, exp-6 *etc.*) a negative thermal expansion is not allowed (Fig. 5*b*). A possible form of the intermolecular potential for the term 2 interaction is indicated schematically in Fig. 5(*c*). It is perhaps surprising that the very simple model used to represent the thermal expansion of the lattice appears to capture the essential chemistry involved in the formation of this complex crystal structure, and that the derived numeric parameters are all reasonable, with contributions from van der Waals forces being weaker than $\pi\cdots\pi$ interactions, followed by hydrogen bonding and then a steric interlock. The Einstein temperatures can also be expressed in kJ mol^{-1}. The van de Waals interactions are modelled by a term of energy 3.2 kJ mol^{-1} (s.u. 0.5), the $\pi\cdots\pi$ 4.4 kJ mol^{-1} (s.u. 0.3), with the hydrogen bonding 7.1 kJ mol^{-1} (s.u. 0.6) and the steric interlock 12.2 kJ mol^{-1} (s.u. 2.8). It is far from clear that these energies correspond directly to bond enthalpies – further research, both theoretical and practical, is required in this direction. That the effective anisotropic Einstein temperatures are high compared with extended network materials (*e.g.* oxides *etc.*) is probably not unreasonable – in solids formed from an infinite network of covalent bonds, the presence of low-energy, cooperative vibrational terms is likely to lower the overall Einstein temperature. Despite its simplicity, this four-interaction model does appear to be fully compatible with the expected chemistry both qualitatively and quantitatively.

In conclusion, the main results of this study are as follows:

(i) it has been demonstrated that analysis of thermal expansion data can yield quantitative and meaningful information about non-covalent intermolecular interactions even for relatively complex molecular solids;

(ii) it has been shown that a simple and intuitive method of indexing a powder diffraction pattern based on variable-temperature studies can be extremely powerful and was invaluable in the present case;

(iii) the crystal structure of glipizide, and the quantitative and directional energies for interactions between molecules have been determined.

The methodology employed is simple, easy to implement and should allow for the straightforward indexing, structure solution and analysis of interactions between molecules for a range of molecular solids.

I wish to acknowledge the support of Jesus College Cambridge through the award of a Junior Research Fellowship.

References

Allen, F. H. (2002). *Acta Cryst.* B**58**, 380–388.
Barron, T. (1955). *Philos. Mag.* **46**, 720–734.

Biernacki, S. & Scheffler, M. (1989). *Phys. Rev. Lett.* **63**, 290–293.
Boultif, A. & Louer, D. (1991). *J. Appl. Cryst.* **24**, 987–993.
Brunelli, M., Wright, J., Vaughan, G., Mora, A. & Fitch, A. (2003). *Angew. Chem. Int. Ed.* **42**, 2029–2032.
David, W., Ibberson, R. & Matsuo, T. (1993). *Proc. R. Soc. London A*, **442**, 129–146.
David, W., Shankland, K., McCusker, L. & Baerlocher, C. (2002). Editors. *International Union of Crystallography Monographs on Crystallography*, No 13. Oxford University Press.
Dunitz, J. & Gavezzotti, A. (2005). *Angew. Chem. Int. Ed.* **44**, 2–23.
Dupont, L., Dideberg, O. & Vermiere, M. (1979). *Acta Cryst.* B**35**, 1501–1504.
Evans, J., Jorgensen, J., Short, S., David, W., Ibberson, R. & Sleight, A. (1999). *Phys. Rev. B: Condens. Matter Mater. Phys.* **60**, 14643–14648.
Finger, L., Cox, D. & Jephcoat, A. (1994). *J. Appl. Cryst.* **27**, 892–900.
Krishnan, R., Srinivasan, R. & Devanarayanan, S. (1979). *Thermal Expansion of Crystals.* Oxford: Pergamon Press.
Larson, A. & Von Dreele, R. B. (1990). *GSAS*. Technical Report LAUR 86-748. Los Alamos National Laboratory.
Le Bail, A., Duroy, H. & Forquest, J. (1988). *Mater. Res. Bull.* **23**, 447–452.
Lommerse, J., Motherwell, W., Ammon, H., Dunitz, J., Gavezzotti, A., Hofmann, D., Leusen, F., Mooij, W., Price, S., Schweizer, B., Schmidt, M., van Eijck, B., Verwer, P. & Williams, D. (2000). *Acta Cryst.* B**56**, 697–714.
Mary, T., Evans, J., Vogt, T. & Sleight, A. (1996). *Science (Washington DC, USA)*, **272**, 90–92.
Munn, R. (1975). *Phys. Rev. B: Condens. Matter Mater. Phys.* **12**, 3491–3493.
Nernst, W. (1991). *Ann. Phys.* **36**, 395–439.
Paufler, P. & Weber, T. (1999). *Eur. J. Mineral.* **11**, 721–730.
Ruffa, A. (1980). *J. Mater. Sci.* **15**, 2258–2267.
Schlenker, J., Gibbs, G. & Boisen, M. (1978). *Acta Cryst.* A**34**, 52–54.
Shankland, K., David, W. & Sivia, D. S. (1997). *J. Mater. Chem.* **7**, 569–572.
Stephens, P. & Huq, A. (2002). *Trans. Am. Cryst. Assoc.* **27**, 127–144.
Stephenson, G. (2000). *J. Pharm. Sci.* **89**, 958–966.
Stephenson, G. A., Pfeiffer, R. R. & Byrn, S. R. (1997). *Int. J. Pharm.* **146**, 93–99.
Wang, K. & Reeber, R. (2000). *Appl. Phys. Lett.* **76**, 2203–2204.
Werner, P., Eriksson, L. & Westdahl, M. (1985). *J. Appl. Cryst.* **18**, 367–370.
Zachariasen, W. H. & Ellinger, F. H. (1963). *Acta Cryst.* **16**, 369–375.
Zallen, R. (1974). *Phys. Rev. B: Condens. Matter Mater. Phys.* pp. 4485–4496.